European Journal of Control 48 (2019) 83–96

Contents lists available at ScienceDirect

European Journal of Control

journal homepage: www.elsevier.com/locate/ejcon

A method to improve an electric vehicle's range: Efficient Cruise Control

Anil K. Madhusudhanan

Department of Engineering, University of Cambridge, Trumpington Street, Cambridge CB2 1PZ, United Kingdom

ARTICLE INFO

Article history:
Received 18 June 2018
Revised 8 October 2018
Accepted 9 December 2018
Available online 13 December 2018

Recommended by Dr H Zhang

Keywords:
Electric vehicle
Energy efficiency
Range anxiety
Traffic signals
Model Predictive Control

ABSTRACT

This article proposes a method to improve the range of an electric vehicle (EV) by controlling its speed depending on the upcoming traffic signal status. A conventional Adaptive Cruise Control (ACC) controls an EV's speed such that there is a certain distance between the EV and the preceding vehicle. However, if the preceding vehicle drives at a non-optimum speed given the upcoming traffic signal status, as it nears the upcoming traffic signal the preceding vehicle will have to dissipate the unnecessarily gained kinetic energy by braking. If the EV blindly follows such a preceding vehicle using a conventional ACC, the EV will also have to dissipate a part of its kinetic energy by braking. In this work, this problem is addressed by proposing an Efficient Cruise Control (ECC). In the proposed ECC, if the EV is within a certain distance of the upcoming traffic signal, its speed reference is calculated based on the traffic signal status, while maintaining a minimum safe inter-vehicular distance from the preceding vehicle. The ECC is designed using Model Predictive Control theory and it is studied in a simulation environment using a Tesla S vehicle model. The simulation results show that the proposed controller improves the EV's energy efficiency and therefore range, where the latter is an important bottleneck in widespread adoption of EVs.

1. Introduction

Carbon emissions is one of the most important challenges of the 21st century. Widespread acceptance of electric vehicle (EV) can contribute towards overcoming this challenge [2,7,12]. One of the main obstacles in widespread acceptance of EVs is range anxiety, where range is the distance an EV can travel from full charge. EVs have limited range as current battery technologies have much lower energy density than conventional energy sources like diesel or petrol [18]. Therefore, improving the energy efficiency and thereby improving the range of an EV is an important research direction that deserves attention. In this context, this article proposes an Efficient Cruise Control (ECC) to improve the range of an EV.

Many of the existing EVs and Internal Combustion Engine based vehicles are equipped with Adaptive Cruise Control (ACC) [14]. It is an Advanced Driver Assistance System (ADAS) that controls distance between a host vehicle and the preceding vehicle. The host vehicle is equipped with ACC and the preceding vehicle is the vehicle directly in front of the host vehicle. Typically, ACC controls the inter-vehicular distance to be proportional to the host vehicle speed [4]. This means as the host vehicle speed increases, the inter-vehicular distance reference increases. At steady state, both the host and preceding vehicles will have the same speed.

As the inter-vehicular distance reference changes with the vehicle speed, the reference is usually transformed to obtain a time-invariant reference and is called time gap. This transformed reference, time gap, is multiplied by the host vehicle speed and then added to a desired standstill inter-vehicular distance to obtain the inter-vehicular distance reference. Typical values of time gap while engaging ACC are 1.5 s, 2.0 s, etc.

However, following the preceding vehicle at a constant time gap may not be energy efficient. If the preceding vehicle travels at a non-optimum speed given the upcoming traffic signal status, *e.g.* while the next traffic signal is red, the preceding vehicle will have to dissipate some of the unnecessarily gained kinetic energy as heat by braking. The following EV will also have to dissipate a part of its kinetic energy by braking if it follows the preceding vehicle. Note that although most EVs have regenerative braking, a significant part of the kinetic energy is not recuperated using regenerative braking [16,17].

In [1], this problem is addressed using a predictive adaptive cruise controller which uses the upcoming traffic signal information to reduce the idle time at traffic lights. However, the vehicle model treats the road disturbance forces such as aerodynamic

E-mail address: ak2102@cam.ac.uk

https://doi.org/10.1016/j.ejcon.2018.12.006

drag force, rolling resistance force and road grade force as available measurements. In addition, the controller's quadratic cost function only aims to minimize braking and does not aim to minimize acceleration. The inter-vehicular minimum safe distance is calculated using a dynamic time gap of 0.2 s. This is 10 times lower than the recommended time gap from the UK Driver and Vehicle Standards Agency [3].

Using traffic information, an energy management strategy for hybrid electric vehicles is proposed in [8] to find the optimal torque split ratio, gear shift schedule and velocity trajectory. The focus is to use a cost function that aims to minimize the energy loss due to aerodynamic drag, rolling resistance, road gradient and braking. Similar to [1], the cost function does not aim to minimize acceleration. In addition, the method does not consider inter-vehicular distance, which makes it unsuitable for situations where the preceding vehicle is close to the host vehicle.

In [20], the authors make an interesting contribution to predict the vehicle queue length while approaching a traffic signal. The prediction of queue length assumes a certain relationship between the vehicle flow and density. As the controller does not measure the inter-vehicular distance directly, but uses the predicted queue length and predicted tail location of the queue, it may not guarantee a minimum safe inter-vehicular distance. Nevertheless, the prediction of queue length is complimentary with this work.

The controller proposed in this article is called Efficient Cruise Control (ECC) and it regulates an EV's speed so that it is more energy efficient than while employing a traditional ACC. In addition to the main measurements a conventional ACC uses, *i.e.* the inter-vehicular distance, vehicle speed and vehicle acceleration, the proposed ECC also uses the upcoming traffic signal status. The upcoming traffic signal status is considered to be available via 3G or 4G mobile communication [6]. The high level ECC objective is to generate a speed reference considering the upcoming traffic signal status and the distance to the upcoming traffic signal, while maintaining a safe minimum inter-vehicular distance from the preceding vehicle.

Compared to the previous work in [1,8,20], this work has the following features.

- The proposed controller uses a vehicle model based on kinematics. The modeling approach is also used in Cooperative Adaptive Cruise Control (CACC), which is experimentally tested and validated on Dutch public roads by TNO Integrated Vehicle Safety Department [13].
- The proposed method uses desired longitudinal acceleration as the control input, which is practical as longitudinal acceleration sensor is present in most commercial vehicles.
- The quadratic cost function in the proposed controller aims to minimize both braking and acceleration.
- The proposed method considers inter-vehicular distance so that the vehicle maintains a safe distance from the preceding vehicle. The controller uses the recommended minimum time gap of 2 s from the UK Driver and Vehicle Standards Agency [3].

This article is structured as follows. In Section 2, the system model used for controller design is introduced. Section 3.1 describes the proposed ECC design, whereas Section 4.1 describes the ACC design used to benchmark the ECC. In Section 5, the proposed controller is evaluated using MATLAB and IPG CarMaker software packages. Section 6 shares the main conclusions of the proposed controller, its potential limitations and future work.

2. System model

The design and implementation of ECC is done using the error dynamics of vehicle speed, error dynamics of inter-vehicular distance and the longitudinal acceleration dynamics. The inter-vehicular distance error, $d_e(t)$, is defined as follows.

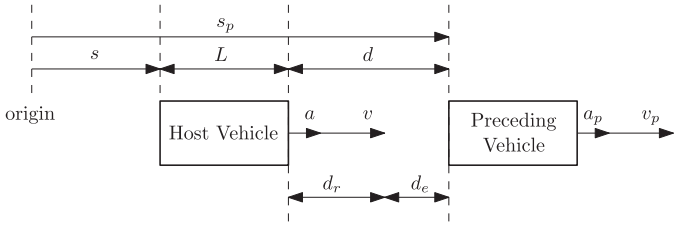

Fig. 1. Schematic diagram showing the system model variables.

$$d_e(t) = d(t) - d_r(t), \text{ where} \tag{1}$$

$$d(t) = s_p(t) - s(t) - L \text{ and} \tag{2}$$

$$d_r(t) = hv(t) + r. \tag{3}$$

Here d is the inter-vehicular distance between the host and preceding vehicles, d_r is the inter-vehicular distance reference of the host vehicle, s_p is the distance travelled by the preceding vehicle, s is the distance travelled by the host vehicle in which the ECC is implemented, L is the length of the host vehicle, h is the time gap, v is the host vehicle speed and r is the desired positive inter-vehicular distance when the host vehicle is at standstill. Many of these variables are shown in Fig. 1.

Using (2) and (3) in (1) and differentiating gives the following equation.

$$\dot{d}_e(t) = v_p(t) - v(t) - ha(t). \tag{4}$$

Here v_p is the preceding vehicle's speed and a is the host vehicle's longitudinal acceleration. The host vehicle speed error, v_e, is defined as follows.

$$v_e(t) = v(t) - v_r(t), \text{ where} \tag{5}$$

$$v_r(t) = \frac{s_{tl}}{t_g}. \tag{6}$$

Here v_r is the host vehicle's speed reference, s_{tl} is the distance of host vehicle to the upcoming traffic signal and t_g is the remaining time after which the host vehicle can pass through the traffic signal. The remaining time, t_g, is calculated using the upcoming traffic signal's current status signals. Note that (6) represents the speed reference with which the host vehicle can approach the upcoming traffic signal without dissipating a considerable amount of its kinetic energy as heat by braking.

Using (5) in (4) gives the following equation.

$$\dot{d}_e(t) = v_p(t) - v_e(t) - v_r(t) - ha(t). \tag{7}$$

Using (6) in (5) and differentiating gives the following equation.

$$\dot{v}_e(t) = a(t) - \frac{\dot{s}_{tl}t_g - \dot{t}_g s_{tl}}{t_g^2}. \tag{8}$$

Note that $\dot{t}_g = -1$ because t_g is the remaining time after which the host vehicle can pass through the traffic signal when the traffic signal state will be green. Therefore, t_g counts down at a rate of one per second. Given $\dot{t}_g = -1$ and considering the reference speed, v_r, as time-invariant, $\dot{s}_{tl} = -v_r$ can be found from (6). Now using $\dot{s}_{tl} = -v_r$ and $\dot{t}_g = -1$, (8) is simplified as follows.

$$\dot{v}_e(t) = a(t) - \frac{v_r t_g + s_{tl}}{t_g^2}. \tag{9}$$

Using (6), (9) is simplified as follows.

$$\dot{v}_e(t) = a(t). \tag{10}$$

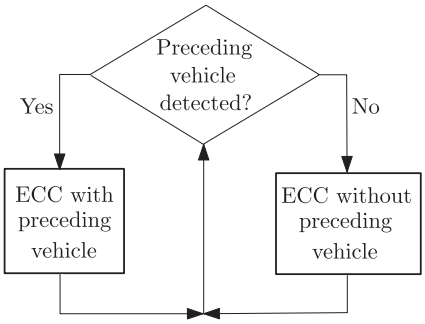

Fig. 2. ECC design with two controllers.

This simplification assumes a time-invariant reference speed, v_r. This is reasonable as v_r does not vary much, as shown in the results section.

The longitudinal acceleration dynamics of the host vehicle is approximated by the following first order differential equation.

$$\dot{a}(t) = -\frac{1}{\tau}a(t) + \frac{1}{\tau}u(t). \tag{11}$$

Here τ is the acceleration time constant and $u(t)$ is the control input of the host vehicle.

Combining (7), (10) and (11) gives the following system model.

$$\begin{bmatrix} \dot{d}_e \\ \dot{v}_e \\ \dot{a} \end{bmatrix} = \begin{bmatrix} 0 & -1 & -h \\ 0 & 0 & 1 \\ 0 & 0 & -\frac{1}{\tau} \end{bmatrix} \begin{bmatrix} d_e \\ v_e \\ a \end{bmatrix} + \begin{bmatrix} 0 \\ 0 \\ \frac{1}{\tau} \end{bmatrix} u \tag{12}$$

$$+ \begin{bmatrix} 1 & -1 \\ 0 & 0 \\ 0 & 0 \end{bmatrix} \begin{bmatrix} v_p \\ v_r \end{bmatrix}. \tag{12}$$

In (12), the time variables in brackets are omitted for simplicity. Combining (4), $\dot{v} = a$ and (11) gives the following system model.

$$\begin{bmatrix} \dot{d}_e \\ \dot{v} \\ \dot{a} \end{bmatrix} = \begin{bmatrix} 0 & -1 & -h \\ 0 & 0 & 1 \\ 0 & 0 & -\frac{1}{\tau} \end{bmatrix} \begin{bmatrix} d_e \\ v \\ a \end{bmatrix} + \begin{bmatrix} 0 \\ 0 \\ \frac{1}{\tau} \end{bmatrix} u + \begin{bmatrix} 1 \\ 0 \\ 0 \end{bmatrix} v_p. \tag{13}$$

Combining (10) and (11) gives the following system model.

$$\begin{bmatrix} \dot{v}_e \\ \dot{a} \end{bmatrix} = \begin{bmatrix} 0 & 1 \\ 0 & -\frac{1}{\tau} \end{bmatrix} \begin{bmatrix} v_e \\ a \end{bmatrix} + \begin{bmatrix} 0 \\ \frac{1}{\tau} \end{bmatrix} u. \tag{14}$$

The system models in (12), (13) and (14) are used in Sections 3.1 and 4.1 to design the control systems.

3. Efficient Cruise Control design

The Efficient Cruise Control (ECC) design consists of two controllers as shown in Fig. 2. These two controllers are designed using Model Predictive Control (MPC) theory. The first MPC is based on the system model in (12), which contains the inter-vehicular distance error as a state, and is used when there is a preceding vehicle in front of the host vehicle. The second MPC is based on the system model in (14), which does not contain the inter-vehicular distance error as a state, and is used when there is no preceding vehicle in front of the host vehicle.

3.1. Control law in the presence of a preceding vehicle

This subsection describes the design of ECC's *ECC with preceding vehicle* block in Fig. 2. The system model in (12) is used to design this control law. The model in (12) is first rewritten as follows.

$$\dot{x} = A_{ct}x + B_{1,ct}u + B_{2,ct}e, \text{ where} \tag{15}$$

$$x = \begin{bmatrix} d_e \\ v_e \\ a \end{bmatrix}, \tag{16}$$

$$A_{ct} = \begin{bmatrix} 0 & -1 & -h \\ 0 & 0 & 1 \\ 0 & 0 & -\frac{1}{\tau} \end{bmatrix}, \tag{17}$$

$$B_{1,ct} = \begin{bmatrix} 0 \\ 0 \\ \frac{1}{\tau} \end{bmatrix}, \tag{18}$$

$$B_{2,ct} = \begin{bmatrix} 1 & -1 \\ 0 & 0 \\ 0 & 0 \end{bmatrix} \text{ and} \tag{19}$$

$$e = \begin{bmatrix} v_p \\ v_r \end{bmatrix}. \tag{20}$$

The $B_{2,ct}e$ term in (15) is seen as disturbance as the host vehicle does not have vehicle-to-vehicle communication to control or measure the preceding vehicle speed. Neglecting the disturbance part, the continuous-time differential equation in (15) is discretised as follows.

$$x(k+1) = Ax(k) + Bu(k). \tag{21}$$

Here A and B are the discrete-time system and input matrices, corresponding to the continuous-time matrices A_{ct} and $B_{1,ct}$ in (15), using a sampling time of 0.01 s. Note that the disturbance part of the model is also neglected in the ACC design in Section 4.1 so that the comparison is fair. Availability of vehicle-to-vehicle communication may increase the performance of the proposed ECC system. However, this is outside the scope of this work.

The following terminal and stage cost functions are used to design the MPC.

$$F(x) = x^T P x, \tag{22}$$

$$L(x,u) = x^T Q x + u^T R u. \tag{23}$$

Here F is the terminal cost, L is the stage cost, P is the terminal state weight, Q is the stage state weight and R is the control input weight. The values of the weighting matrices are $P = \begin{bmatrix} 1 & 0 & 0 \\ 0 & 250 & 0 \\ 0 & 0 & 1 \end{bmatrix}$, $Q = P$ and $R = 1$. From these weighting matrices, it can be observed that the host vehicle speed error state carries the highest weight as following the speed reference is needed to reduce the energy consumption. The MPC design described in this subsection is an adaption of the standard MPC design from [9] for the system described in Section 2.

Considering a prediction horizon of N, the following control input sequence and state sequence are considered.

$$U = \begin{bmatrix} u_0 \\ u_1 \\ \vdots \\ u_{N-1} \end{bmatrix}, X = \begin{bmatrix} x_1 \\ x_2 \\ \vdots \\ x_N \end{bmatrix}. \tag{24}$$

Here u_0 to u_{N-1} are the control inputs at sample 0 to $N-1$, and x_1 to x_N are the system state vectors at sample 1 to N. Using (21) and (24), the state sequence, X, is written using the prediction matrices, Φ and Γ, as follows.

$$X = \Phi x_0 + \Gamma U, \text{ where} \tag{25}$$

$$\Phi = \begin{bmatrix} A \\ A^2 \\ \vdots \\ A^N \end{bmatrix} \text{ and} \tag{26}$$

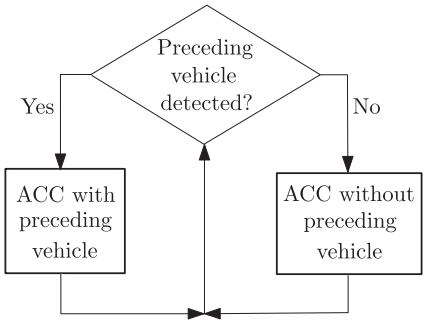

Fig. 3. ACC design with two controllers.

$$\Gamma = \begin{bmatrix} B & 0 & \cdots & 0 \\ AB & B & \cdots & 0 \\ \vdots & \vdots & \ddots & \vdots \\ A^{N-1}B & A^{N-2}B & \cdots & B \end{bmatrix}. \tag{27}$$

The cost function to minimize, $V(x_0, U)$, is written as follows using the terminal and stage cost functions in (22) and (23).

$$V(x_0, U) = F(x_N) + \sum_{i=0}^{N-1} L(x_i, u_i) \tag{28}$$

$$= x_N^T P x_N + \sum_{i=0}^{N-1} x_i^T Q x_i + u_i^T R u_i. \tag{29}$$

Note that in (29), the terms with $i < N$ are the quadratic costs for the state vectors and control inputs before the last sample in the MPC prediction horizon, whereas the term with $i = N$ is the quadratic cost for the state vector at the last sample in the prediction horizon [9]. At $i = N$, there is no cost for the control input as $i = N$ represents the last sample in the prediction horizon, where the system is at the terminal state.

The cost function, $V(x_0, U)$, is rewritten using the matrices Ω and Ψ as follows.

$$V(x_0, U) = x_0^T Q x_0 + X^T \Omega X + U^T \Psi U, \text{ where} \tag{30}$$

$$\Omega = \begin{bmatrix} Q & & & & \\ & Q & & & \\ & & \ddots & & \\ & & & Q & \\ & & & & P \end{bmatrix} \text{ and} \tag{31}$$

$$\Psi = \begin{bmatrix} R & & & \\ & R & & \\ & & \ddots & \\ & & & R \end{bmatrix}. \tag{32}$$

Using Ψ, Γ, Ω and Φ, matrices G and F are now defined as follows.

$$G = 2\left(\Psi + \Gamma^T \Omega \Gamma\right), \tag{33}$$

$$F = 2\Gamma^T \Omega \Phi. \tag{34}$$

Using (25), (33) and (34) in (30) and rearranging gives the following equation for the cost function, $V(x_0, U)$.

$$V(x_0, U) = \frac{1}{2} U^T G U + U^T F x_0 + x_0^T \left(Q + \Phi^T \Omega \Phi\right) x_0. \tag{35}$$

For the MPC problem with a vehicle in front of the host vehicle, the following constraints are considered for the control input and the inter-vehicular distance error.

$$u_{\min} \le u \le u_{\max}, \tag{36}$$

$$d_e \ge d_{e,\,\min}. \tag{37}$$

Here $u_{\min}$ is the lower limit of control input, $u_{\max}$ is the upper limit of control input and $d_{e,\min}$ is the lower limit of inter-vehicular distance error. Using the constraints in (36) and (37), the stage and terminal constraints of the MPC problem are written as follows.

$$M_i x_i + E_i u_i \le b_i, \text{ where } i = 0, 1, \ldots, N-1, \tag{38}$$

$$M_N x_N \le b_N. \text{ Here} \tag{39}$$

$$M_i = \begin{bmatrix} 0 & 0 & 0 \\ 0 & 0 & 0 \\ -1 & 0 & 0 \end{bmatrix}, \tag{40}$$

$$E_i = \begin{bmatrix} 1 \\ -1 \\ 0 \end{bmatrix}, \tag{41}$$

$$b_i = \begin{bmatrix} u_{\max} \\ -u_{\min} \\ -d_{e,\min} \end{bmatrix}, \tag{42}$$

$$M_N = \begin{bmatrix} -1 \\ 0 \\ 0 \end{bmatrix} \text{ and} \tag{43}$$

$$b_N = -d_{e,\,\min}. \tag{44}$$

The inequalities in (38) and (39) are now combined to generate a Linear Matrix Inequality (LMI) as shown below.

$$Dx_0 + MX + \epsilon U \le c, \text{ where} \tag{45}$$

$$D = \begin{bmatrix} M_0 \\ 0 \\ \vdots \\ 0 \end{bmatrix}, \tag{46}$$

$$M = \begin{bmatrix} 0 & \cdots & 0 \\ M_1 & \cdots & 0 \\ \vdots & \ddots & \vdots \\ 0 & \cdots & M_N \end{bmatrix}, \tag{47}$$

$$\epsilon = \begin{bmatrix} E_0 & \cdots & 0 \\ \vdots & \ddots & \vdots \\ 0 & \cdots & E_{N-1} \\ 0 & \cdots & 0 \end{bmatrix} \text{ and} \tag{48}$$

$$c = \begin{bmatrix} b_0 \\ b_1 \\ \vdots \\ b_N \end{bmatrix}. \tag{49}$$

Using (25), the LMI in (45) is rewritten as follows.

$$Dx_0 + M\Phi x_0 + M\Gamma U + \epsilon U \le c. \tag{50}$$

Using $J = M\Gamma + \epsilon$ and $W = -D - M\Phi$, the LMI in (50) is rewritten as shown below.

$$JU \le c + W x_0. \tag{51}$$

The MPC problem is now written using the cost function, $V(x_0, U)$, in (35) and the constraints in (51) as follows.

$$\begin{aligned} \underset{U}{\text{minimize}} \quad & \frac{1}{2}U^T GU + U^T F x_0, \\ \text{subject to} \quad & JU \leq c + W x_0. \end{aligned} \tag{52}$$

The above MPC problem can be solved using a quadratic programming function, *e.g.* the *quadprog* function in MATLAB. The control input in the current sample time, $u(x_0)$, is now defined as follows, where U^* is the solution of (52).

$$u(x_0) = \begin{bmatrix} I & 0 & \cdots & 0 \end{bmatrix} U^*(x_0). \tag{53}$$

Using the quadratic cost of host vehicle speed error in (22) and (23), and the constraint of inter-vehicular distance error in (37), the MPC problem generates the control input in the presence of a preceding vehicle such that the host vehicle speed error magnitude is minimized as much as possible, while maintaining a safe minimum inter-vehicular distance.

3.2. Control law in the absence of a preceding vehicle

This subsection describes the design of ECC's *ECC without preceding vehicle* block in Fig. 2. The system model in (14) is used to design this control law. The model in (14) is first rewritten as follows.

$$\dot{x} = A_{ct}x + B_{ct}u, \text{ where} \tag{54}$$

$$x = \begin{bmatrix} v_e \\ a \end{bmatrix}, \tag{55}$$

$$A_{ct} = \begin{bmatrix} 0 & 1 \\ 0 & -\frac{1}{\tau} \end{bmatrix} \text{ and} \tag{56}$$

$$B_{ct} = \begin{bmatrix} 0 \\ \frac{1}{\tau} \end{bmatrix}. \tag{57}$$

There is no inter-vehicular distance error state as there is no preceding vehicle. The continuous-time differential equation in (54) is discretised as follows.

$$x(k+1) = Ax(k) + Bu(k). \tag{58}$$

Here A and B are the discrete-time system and input matrices, corresponding to the continuous-time matrices A_{ct} and B_{ct} in (54), using a sampling time of 0.01 s.

For the MPC design without a vehicle in front of the host vehicle, the following control input constraints are considered.

$$u_{\min} \leq u \leq u_{\max}. \tag{59}$$

Using the system model in (58) and the system constraints in (59), the same procedure, described in equations (22) to (53), is followed to generate the MPC control input when there is no preceding vehicle.

4. Adaptive Cruise Control design

An Adaptive Cruise Control (ACC) is used to benchmark the proposed ECC. Similar to ECC, the ACC design consists of two controllers as shown in Fig. 3. These two controllers are also based on Model Predictive Control (MPC) theory. Similar to the ECC design, the first MPC is based on the system model in (13), which contains the inter-vehicular distance error as a state, and is used when there is a vehicle in front of the host vehicle. The second MPC acts as a cruise control and is used when there is no vehicle in front of the host vehicle. Similar to ECC, MPC theory is used to design the ACC so that the comparison between ECC and ACC does not suffer from different control theories.

4.1. Control law in the presence of a preceding vehicle

This subsection describes the design of ACC's *ACC with preceding vehicle* block in Fig. 3. The system model in (13) is used to design this control law. The model in (13) is first rewritten as follows.

$$\dot{x} = A_{ct}x + B_{1,ct}u + B_{2,ct}v_p, \text{ where} \tag{60}$$

$$x = \begin{bmatrix} d_e \\ v \\ a \end{bmatrix}, \tag{61}$$

$$A_{ct} = \begin{bmatrix} 0 & -1 & -h \\ 0 & 0 & 1 \\ 0 & 0 & -\frac{1}{\tau} \end{bmatrix}, \tag{62}$$

$$B_{1,ct} = \begin{bmatrix} 0 \\ 0 \\ \frac{1}{\tau} \end{bmatrix} \text{ and} \tag{63}$$

$$B_{2,ct} = \begin{bmatrix} 1 \\ 0 \\ 0 \end{bmatrix}. \tag{64}$$

The $B_{2,ct}v_p$ term in (60) is seen as disturbance as the host vehicle does not have vehicle-to-vehicle communication to control or measure the preceding vehicle speed. Neglecting the disturbance part, the continuous-time differential equation in (60) is discretised as follows.

$$x(k+1) = Ax(k) + Bu(k). \tag{65}$$

Note that the disturbance part of the model is also neglected in the ECC design in Section 3.1 so that the comparison is fair. Extending the ACC design to a CACC system with vehicle-to-vehicle communication may increase the performance as it can reduce the control effort and thereby reduce energy consumption [13,19]. However, this is outside the scope of this work.

For the MPC design with a vehicle in front of the host vehicle, the following constraints are considered for the control input, vehicle speed and the inter-vehicular distance.

$$u_{\min} \leq u \leq u_{\max}, \tag{66}$$

$$v_{\min} \leq v \leq v_{\max}, \tag{67}$$

$$d \geq d_{\min}. \tag{68}$$

Using the system model in (65) and the system constraints in (66)–(68), the same procedure, described in Eqs. (22)–(53), is followed to generate the MPC control input when there is a preceding vehicle.

4.2. Control law in the absence of a preceding vehicle

In the absence of a preceding vehicle, the ACC's control law is that of a cruise control. Therefore, the same controller in 3.2 is used for this case. The only difference is that the vehicle reference speed is the upper speed limit, *i.e.* $v_r = v_{\max}$.

5. Evaluation of Efficient Cruise Control

This section describes evaluation of the proposed ECC. As shown in Fig. 4, the evaluation is performed using a simulation environment using MATLAB and IPG CarMaker software packages. The *Host VM* block in Fig. 4 represents the host vehicle model and the *Preceding VM* block represents the preceding vehicle model. A built-in electric vehicle model of Tesla S in IPG CarMaker is used in this work for both the host vehicle and the preceding vehicle.

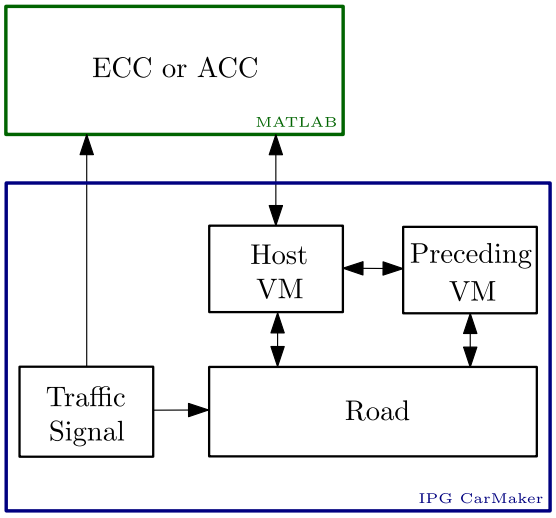

Fig. 4. The simulation environment using MATLAB and IPG CarMaker software packages.

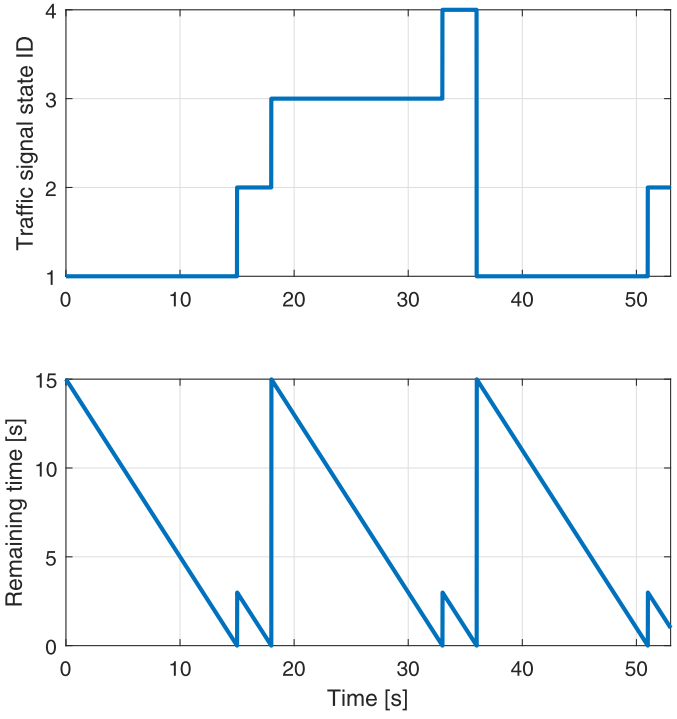

Fig. 5. The traffic signal state ID and the amount of time remaining in the current state, as a function of time, during a simulation with the initial traffic signal state green.

Table 1
The electric vehicle model parameters.

Parameter	Value
Wheelbase	2.9591 m
Track width	1.668 m
Curb weight	2108 kg
Battery pack capacity	84 kWh
Electric machine efficiency	0.78–0.98%
Electric motor maximum power	310 kW

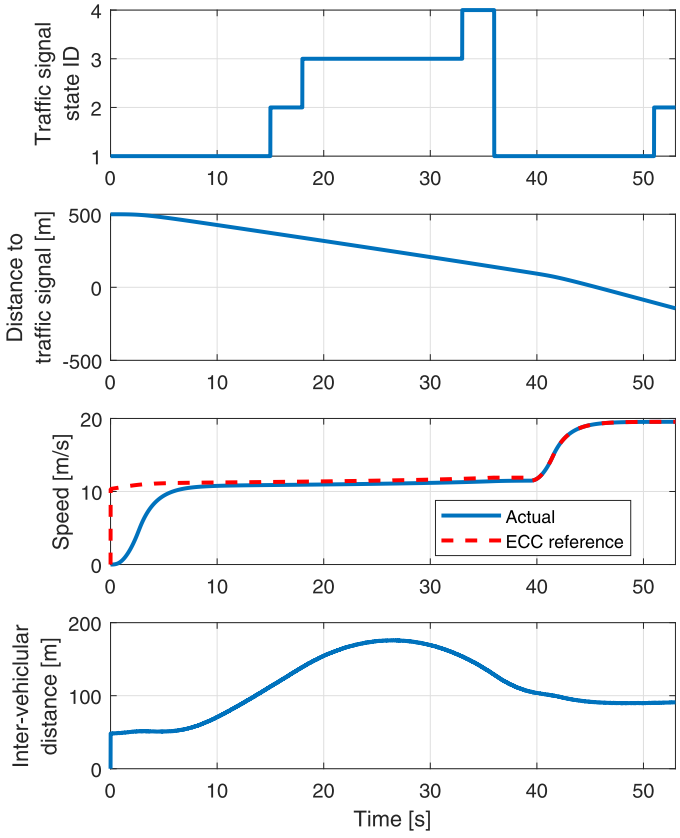

Fig. 6. The traffic signal state ID, and the host vehicle's distance to traffic signal, speed, speed reference and the inter-vehicular distance during a simulation with two vehicles, where the host vehicle uses the proposed ECC and the initial traffic signal state is green.

Table 2
Durations of the traffic signal states.

State	State ID	Duration [s]
Green	1	15
Yellow	2	3
Red	3	15
Red and yellow	4	3

The electric vehicle model parameters are shown in Table 1. In order to benchmark the proposed ECC from Section 3.1, its performance is compared with that of the ACC from Section 4.1. As seen in Sections 3.1 and 4.1, both the ECC and ACC designs are based on the same control theory, MPC, so that their comparison is fair.

The evaluation has two cases. In the first case, the simulations consist of a host vehicle and a preceding vehicle crossing a traffic signal. In the second case, the simulations only consist of a host vehicle crossing a traffic signal. In both cases, the host vehicle performance is evaluated under different initial conditions of the upcoming traffic signal. The host vehicle performance is also evaluated under different initial conditions of the host vehicle speed, preceding vehicle speed and the inter-vehicular distance.

The traffic signal has four states, namely green, yellow, red, and red and yellow. The traffic signal states have different durations as shown in Table 2. The traffic signal state rotates through the different states mentioned in Table 2 continuously. This implies that the sequence of traffic signal state is green, yellow, red, red and yellow, and then again green, etc. The traffic signal status signals are considered to be available via 3G or 4G mobile communication in the host vehicle. The status signals include the current state identifi-

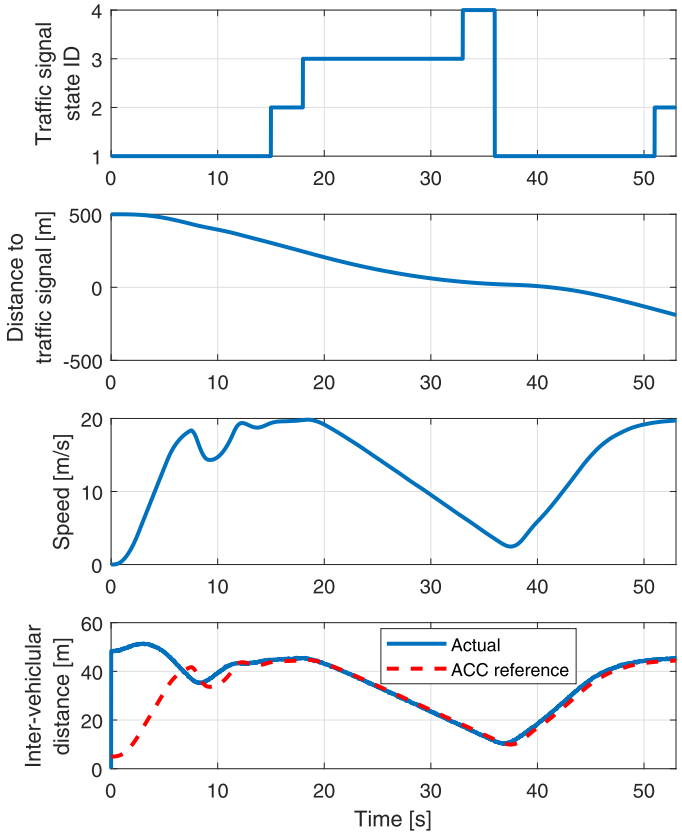

Fig. 7. The traffic signal state ID, and the host vehicle's distance to traffic signal, speed, inter-vehicular distance reference and the inter-vehicular distance during a simulation with two vehicles, where the host vehicle uses the ACC and the initial traffic signal state is green.

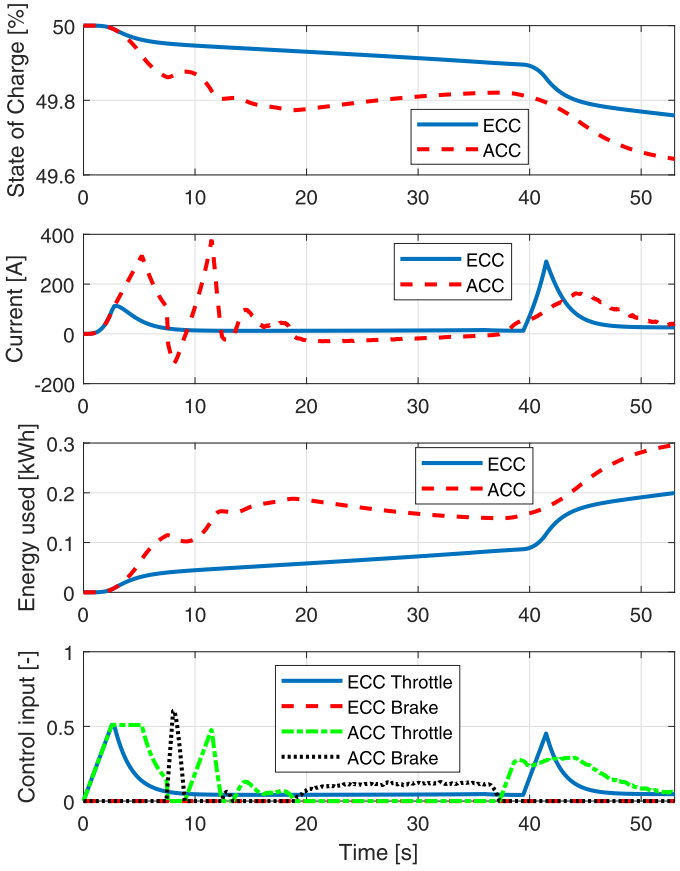

Fig. 8. Performance comparison of the proposed ECC with the ACC during a simulation with two vehicles, where the initial traffic signal state is green.

cation (ID) and the amount of time remaining in the current state. The state ID of each of the states is shown in Table 2.

5.1. Simulation results with two vehicles

In the case with two vehicles, the host vehicle is equipped with either the ACC or the proposed ECC. Therefore, the host vehicle's longitudinal dynamics is controlled by the ACC or ECC but its lateral dynamics is controlled by a built-in driver model in the IPG CarMaker. The maximum lateral acceleration of the IPG driver model is 4 m/s^2. The host vehicle has an initial speed of 0 m/s. Both the host and preceding vehicles travel a distance of 700 m and the traffic signal is at a distance of 500 m from the host vehicle's initial position.

The preceding vehicle's longitudinal and lateral dynamics are controlled by an autonomous driving mode in the IPG CarMaker software. The preceding vehicle has an initial position of 50 m in front of the host vehicle and has an initial speed of 0 m/s. The autonomous driving mode's maximum speed limit is 20 m/s, maximum longitudinal acceleration while cruising or following is 2 m/s^2, minimum longitudinal acceleration while cruising is −5 m/s^2, minimum longitudinal acceleration while following is −9.81 m/s^2 and the maximum lateral acceleration while cruising or following is 4 m/s^2. Here cruising refers to the situation where there is no vehicle in front of the preceding vehicle, whereas following refers to the situation where there is a vehicle in front of the preceding vehicle. In this work, only cruising situations are considered for the preceding vehicle. Note that the minimum longitudinal acceleration of −9.81 m/s^2 is possible in dry road conditions in the absence of lateral dynamics [10,11] and this article does not consider combined tyre slip situations.

In all the simulations, before the host vehicle crosses the traffic signal, the longitudinal dynamics is controlled by either the proposed ECC or the ACC, whereas after the host vehicle crosses the traffic signal, the longitudinal dynamics is always controlled by the ACC. This is because the proposed ECC is only active within a certain distance, in this work 500 m, of the upcoming traffic signal.

In the first simulation, the traffic signal's initial state is green. Fig. 5 shows the traffic signal status signals, *i.e.* the current state ID and the amount of time remaining in the current state, as a function of time. From Fig. 5, it can be seen that the traffic signal state ID starts with 1, *i.e.* state green, and rotates through the different states shown in Table 2. Initially, the amount of time remaining in the current state is 15 s as the initial state ID is 1, *i.e.* state green. Then it reduces and becomes zero when the simulation time reaches 1 s. At this time, the state ID changes from 1 to 2, *i.e.* the state changes from green to yellow. For the state yellow, the duration is 3 s as shown in Table 2. This process continues with the different traffic signal states. Fig. 6 shows the simulation results of the host vehicle using the proposed ECC with the initial traffic signal state green. Fig. 7 shows the simulation results using the ACC. Fig. 8 shows the simulation results, comparing the performances of the proposed ECC and the ACC.

From Figs. 6–8, the following observations can be made.

- The host vehicle with ECC accelerates from standstill and tracks the ECC speed reference (Fig. 6). On the other hand, the host vehicle with ACC accelerates from standstill and tracks the ACC inter-vehicular distance reference (Fig. 7).

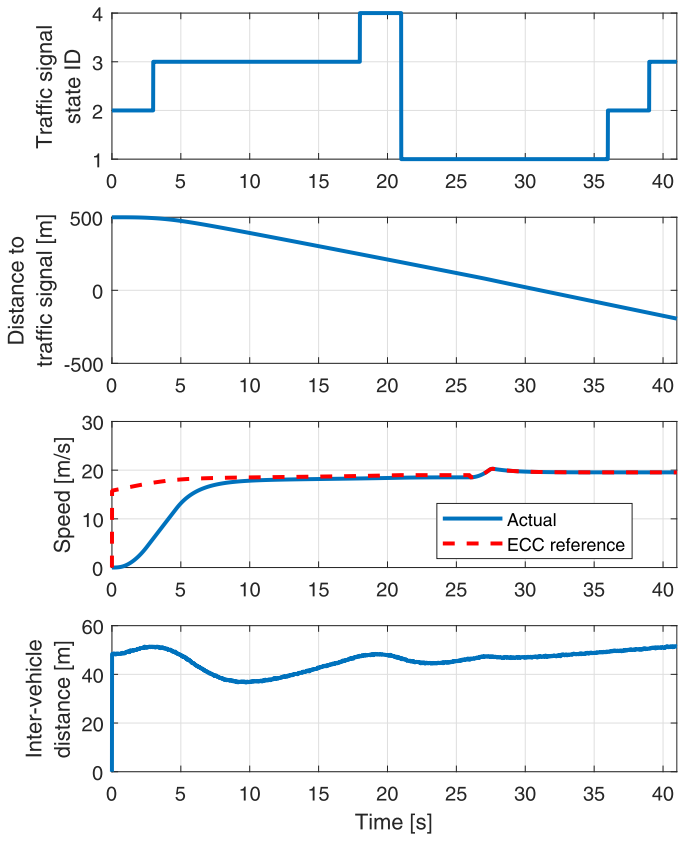

Fig. 9. The traffic signal state ID, and the host vehicle's distance to traffic signal, speed, speed reference and the inter-vehicular distance during a simulation with two vehicles, where the host vehicle uses the proposed ECC and the initial traffic signal state is yellow.

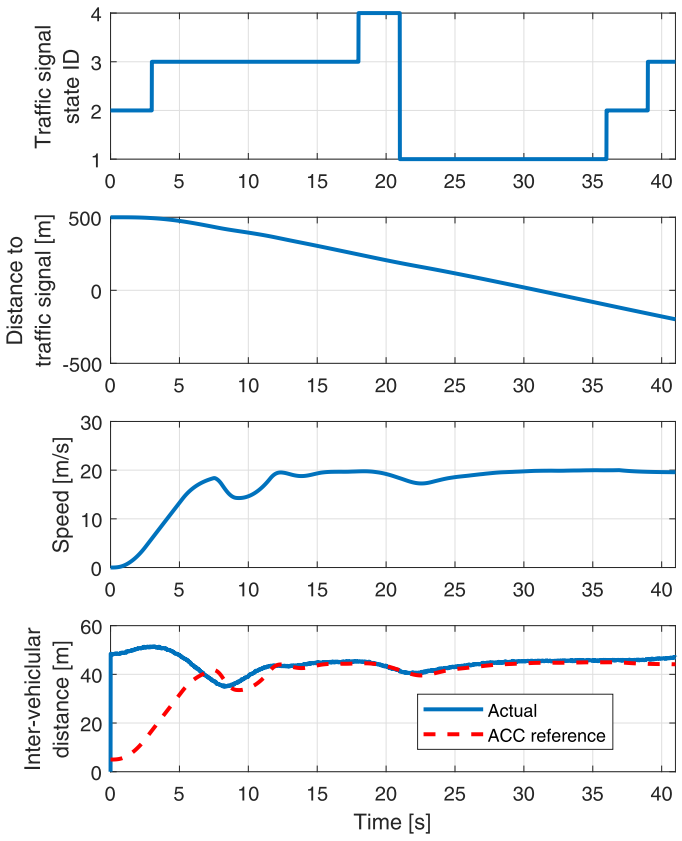

Fig. 10. The traffic signal state ID, and the host vehicle's distance to traffic signal, speed, inter-vehicular distance reference and the inter-vehicular distance during a simulation with two vehicles, where the host vehicle uses the ACC and the initial traffic signal state is yellow.

- In the ECC case, when the distance to the traffic signal approaches 0 m (Fig. 6), the traffic signal state is green (state ID 1) without the host vehicle decelerating. On the other hand, the host vehicle with ACC has to decelerate while the distance to the traffic signal approaches 0 m so that the traffic signal status becomes green (Fig. 7).
- Before the distance to traffic signal becomes 0 m, the speed of the host vehicle with ECC does not vary much (Fig. 6) and does not become as high as the ACC case. On the other hand, the host vehicle with ACC accelerates to 20 m/s and later decelerates to 2.5 m/s (Fig. 7).
- The unnecessary acceleration in the ACC case causes high electric current above 350 A, whereas using ECC, the electric current stays below 150A before the traffic signal (Fig. 8). High electric current is known to reduce an electric vehicle's battery pack efficiency and life span.
- Using the proposed ECC, the battery pack's State of Charge reduction is lower than the ACC case (Fig. 8) before crossing the traffic signal and at the end of the 700 m drive.
- Using the proposed ECC, the electric energy consumption is lower than the ACC case (Fig. 8) before crossing the traffic signal and at the end of the 700 m drive. This means the proposed ECC improves the electric vehicle's energy efficiency.

In the ACC case, as the host vehicle decelerates while approaching the traffic signal, a part of the gained kinetic energy is lost as heat due to friction brakes and only a part of the kinetic energy is recovered using regenerative braking. But using the proposed ECC, kinetic energy is not lost as the vehicle approaches the traffic signal when the traffic signal is green.

Figs. 9–11 show the simulation results with the initial traffic signal state yellow. In this case, the host vehicle speed profiles are comparable using ECC and ACC (Figs. 9 and 10). This happens because the traffic signal becomes green by chance when the host vehicle reaches the traffic signal. It is also seen that the electric energy consumption using ECC is slightly lower than the case with ACC (Fig. 11). The slightly higher electricity consumption using ACC is mainly caused by the braking events around 8 s and 21 s.

Figs. 12–14 show the simulation results with the initial traffic signal state red. In this case, before the traffic signal, the host vehicle travels at a lower speed with ECC compared to the case with ACC (Figs. 12 and 13). This results in a lower energy consumption for the ECC case. An interesting observation is seen in Fig. 14 around 8 s where the ACC applies brakes to maintain the inter-vehicular distance reference, whereas the ECC case does not do that as the ECC does not require the host vehicle to follow the preceding vehicle at an inter-vehicle distance reference. The ECC only requires the host vehicle to keep a minimum positive inter-vehicular distance.

Figs. 15–17 show the simulation results with the initial traffic signal state red and yellow. In this case, the proposed ECC results in considerably lower electricity consumption compared to the ECC case (Fig. 17). This is caused by the host vehicle with ACC coming to an almost standstill (Fig. 16) around 40 s to wait for the traffic signal to become green. On the other hand, ECC makes the host vehicle to travel at an energy efficient speed so that the host vehicle does not have to come to a standstill before crossing the traffic signal (Fig. 15).

Further simulations are performed under three initial conditions with different host vehicle initial speeds, three initial con-

Table 3
Comparison of energy consumption under different initial conditions. The initial traffic signal state is green.

Initial v [m/s]	Initial v_p [m/s]	Initial d [m]	Without ECC [kWh]	With ECC [kWh]	Difference [%]
10	15	25	0.3004	0.2185	-27.26
15	15	35	0.2565	0.2063	-19.57
20	15	45	0.2135	0.1705	-20.14
20	20	15	0.3046	0.1704	-44.06
20	20	30	0.2814	0.1704	-39.45
20	20	45	0.2068	0.1705	-17.55
10	10	25	0.2938	0.2185	-25.63
15	15	35	0.2565	0.2063	-19.57
20	20	45	0.2068	0.1705	-17.55

Table 4
Comparison of energy consumption with and without the proposed ECC.

Initial traffic signal	Preceding vehicle	Without ECC [kWh]	With ECC [kWh]	Difference [%]
Green	Present	0.2922	0.2077	-28.92
Yellow	Present	0.2585	0.2191	-15.24
Red	Present	0.2480	0.2138	-13.79
Red and yellow	Present	0.3008	0.2069	-31.22
Green	Absent	0.3040	0.2111	-30.56
Red	Absent	0.2269	0.2205	-02.82

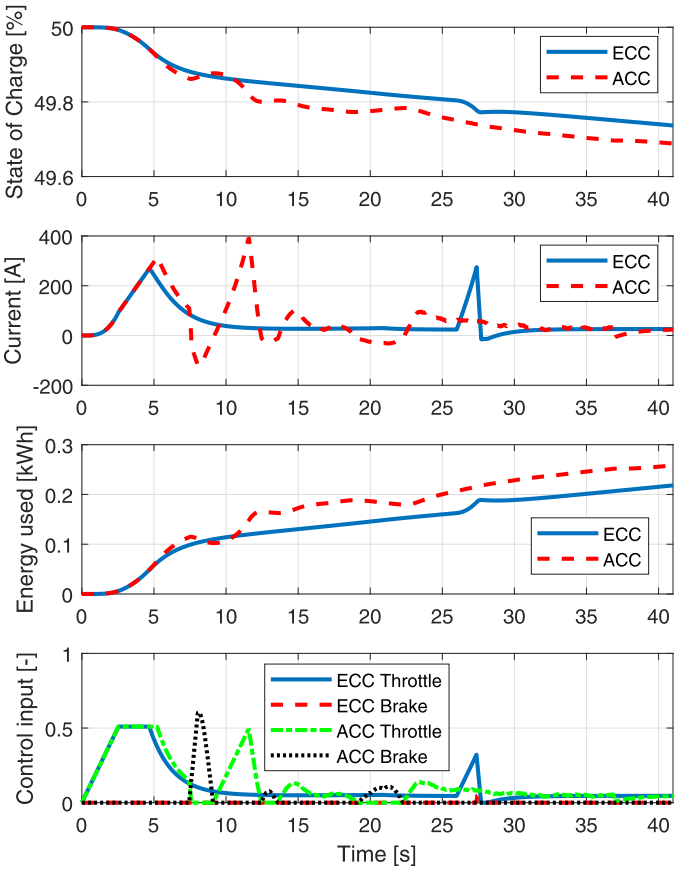

Fig. 11. Performance comparison of the proposed ECC with the ACC during a simulation with two vehicles, where the initial traffic signal state is yellow.

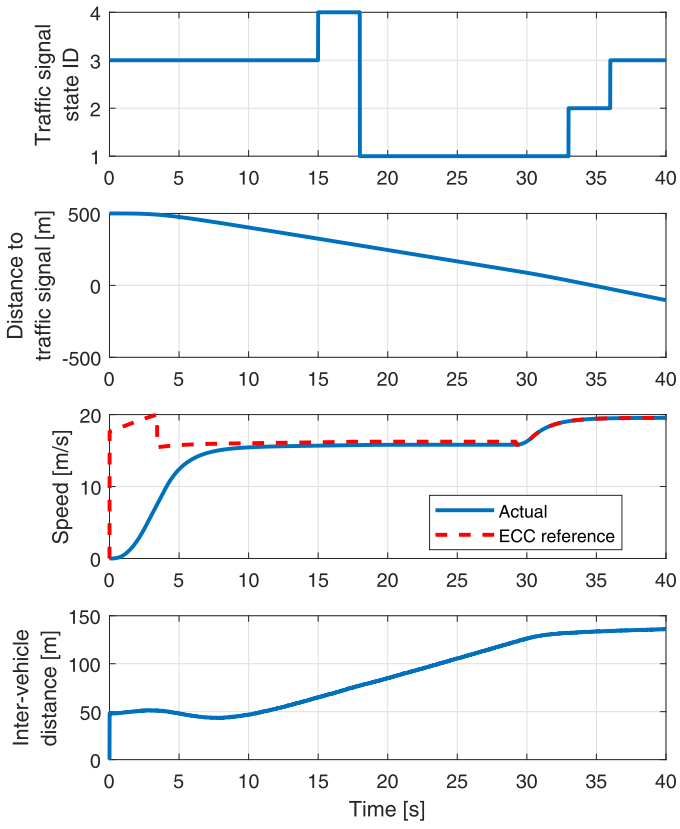

Fig. 12. The traffic signal state ID, and the host vehicle's distance to traffic signal, speed, speed reference and the inter-vehicular distance during a simulation with two vehicles, where the host vehicle uses the proposed ECC and the initial traffic signal state is red.

ditions with different initial positions, and three initial conditions with different host vehicle and preceding vehicle initial speeds. Table 3 shows the electric vehicle's energy consumption with and without the proposed ECC under these initial conditions. The *Difference* column shows percentage energy consumption reduction with the ECC.

Note that the first three rows of the table have different host vehicle initial speeds. The preceding vehicle's initial speed remains the same and the initial inter-vehicular distance is governed by (3). The second three rows of the table have different initial inter-vehicular distances, whereas the host vehicle and preceding vehicle initial speeds are kept constant. The last three rows of the table have different initial speeds for the host and preceding vehicles. Note that in each of the last three rows, the host and preceding vehicles initial speeds are equal and the initial inter-vehicular distance is governed by (3). From Table 3, on average, it is deduced

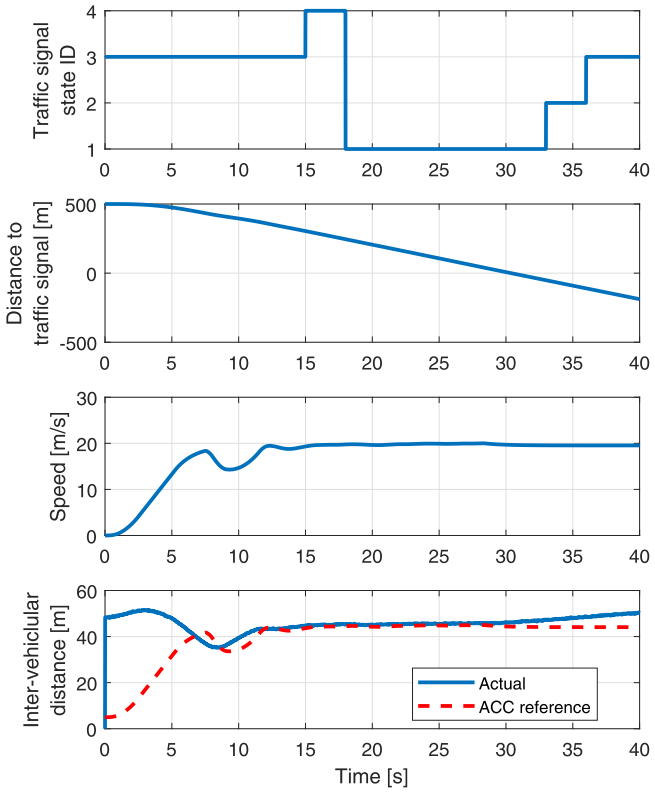

Fig. 13. The traffic signal state ID, and the host vehicle's distance to traffic signal, speed, inter-vehicular distance reference and the inter-vehicular distance during a simulation with two vehicles, where the host vehicle uses the ACC and the initial traffic signal state is red.

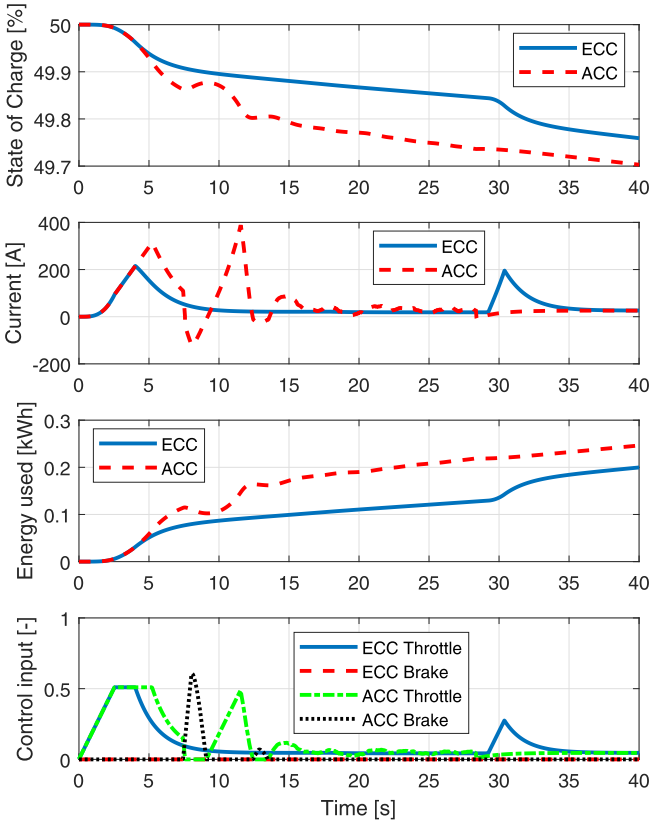

Fig. 14. Performance comparison of the proposed ECC with the ACC during a simulation with two vehicles, where the initial traffic signal state is red.

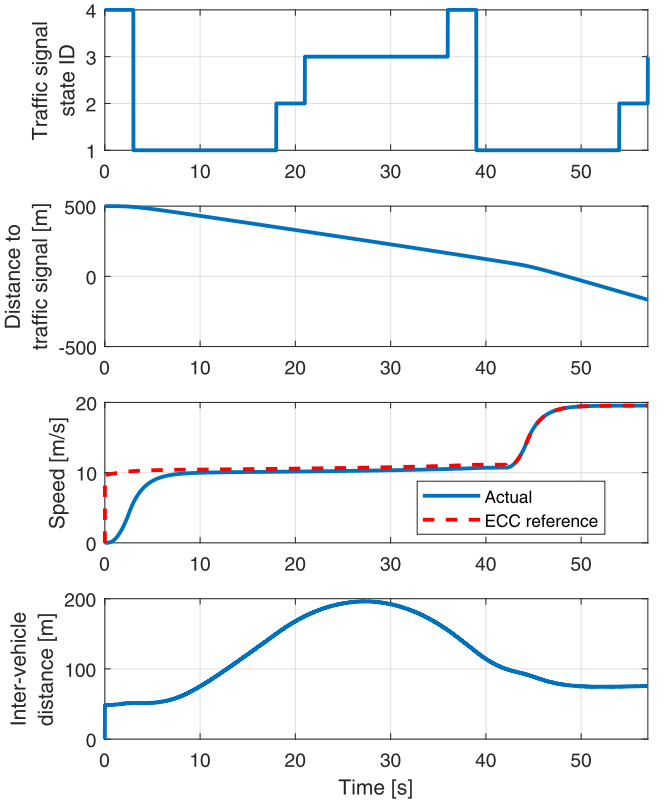

Fig. 15. The traffic signal state ID, and the host vehicle's distance to traffic signal, speed, speed reference and inter-vehicular distance during a simulation with two vehicles, where the host vehicle uses the proposed ECC and the initial traffic signal state is red and yellow.

that the proposed ECC reduces the electric vehicle's energy consumption by approximately 25.64% in the simulations performed.

From all the simulation results in the presence of a preceding vehicle, overall it is seen that the proposed ECC increases energy efficiency of the host vehicle, while compared with the ACC.

Next, simulation studies are performed again for different initial traffic signal conditions, but in the absence of a preceding vehicle.

5.2. Simulation results with one vehicle

In the case with only one vehicle, the host vehicle's longitudinal dynamics is controlled by either the proposed ECC or the driver model in IPG CarMaker. The host vehicle has an initial speed of 0 m/s. The host vehicle travels a distance of 700 m and the traffic signal is at a distance of 500 m from the host vehicle's initial position. The driver model's maximum speed limit is 20 m/s, maximum longitudinal acceleration is 2 m/s^2 and the minimum longitudinal acceleration is -9.81 m/s^2.

In the first simulation without a preceding vehicle, the traffic signal's initial state is green. Fig. 5 shows the traffic signal status signals, *i.e.* the current state ID and the amount of time remaining in the current state, as a function of time.

Fig. 18 shows the simulation results using the proposed ECC with the initial traffic signal state green. Fig. 19 shows the simulation results using the IPG CarMaker driver model. Fig. 20 shows the simulation results, comparing performance of the proposed ECC against the IPG CarMaker driver model. From Figs. 18–20, the following observations can be made.

- Using ECC, the host vehicle accelerates from standstill and tracks the ECC speed reference (Fig. 18). On the other hand, the

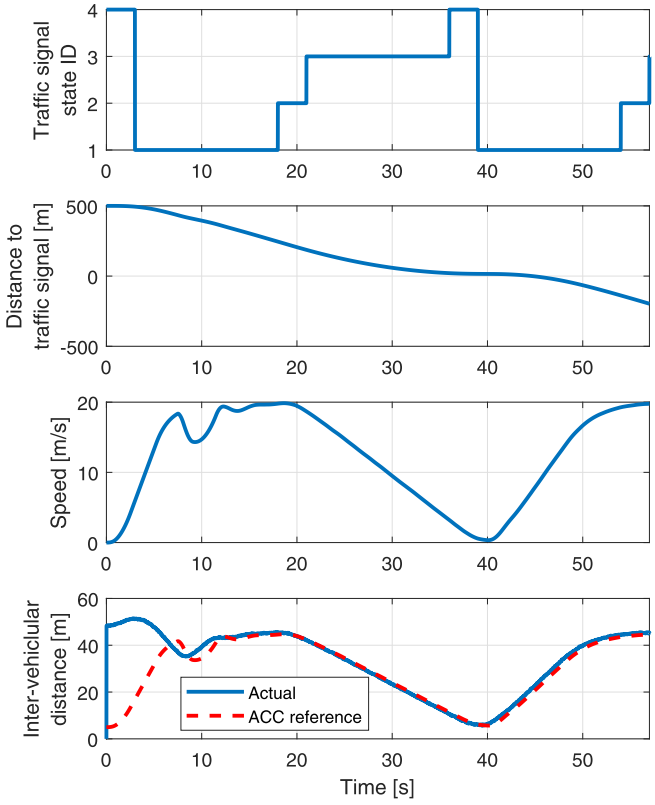

Fig. 16. The traffic signal state ID, and the host vehicle's distance to traffic signal, speed, inter-vehicular distance reference and inter-vehicular distance during a simulation with two vehicles, where the host vehicle uses the ACC and the initial traffic signal state is red and yellow.

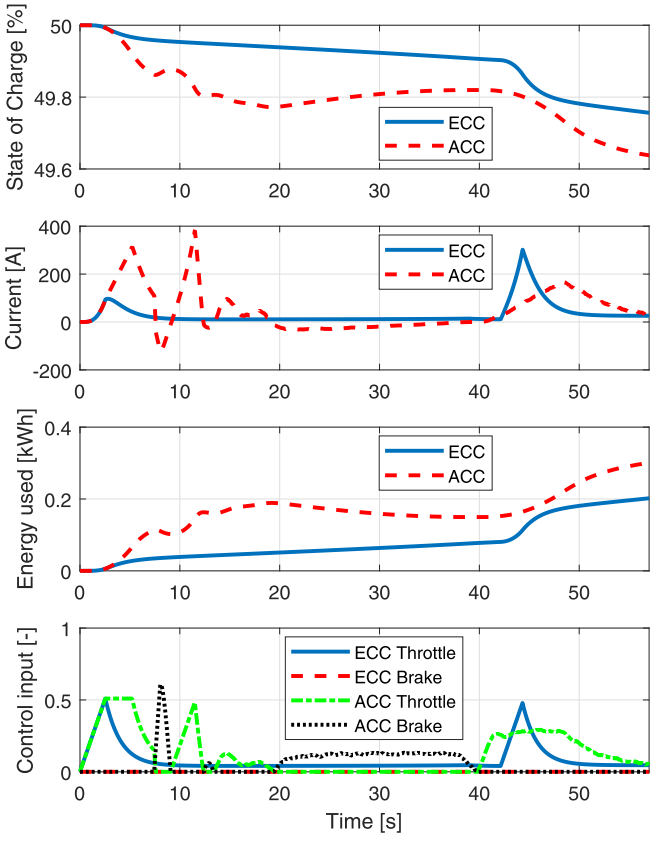

Fig. 17. Performance comparison of the proposed ECC with the ACC during a simulation with two vehicles, where the initial traffic signal state is red and yellow.

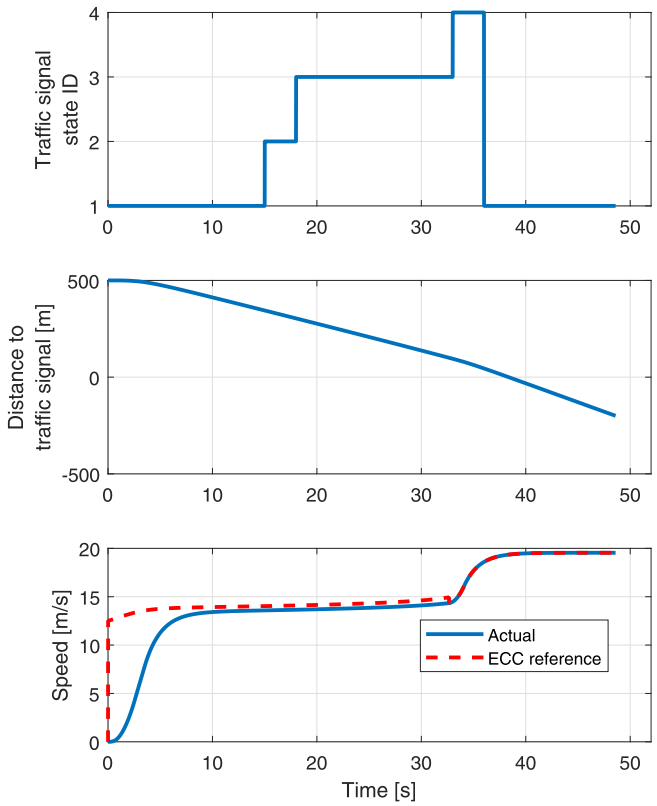

Fig. 18. The traffic signal state ID, and the host vehicle's distance to traffic signal, speed and the speed reference during a simulation without a preceding vehicle, where the host vehicle uses the proposed ECC and the initial traffic signal state is green.

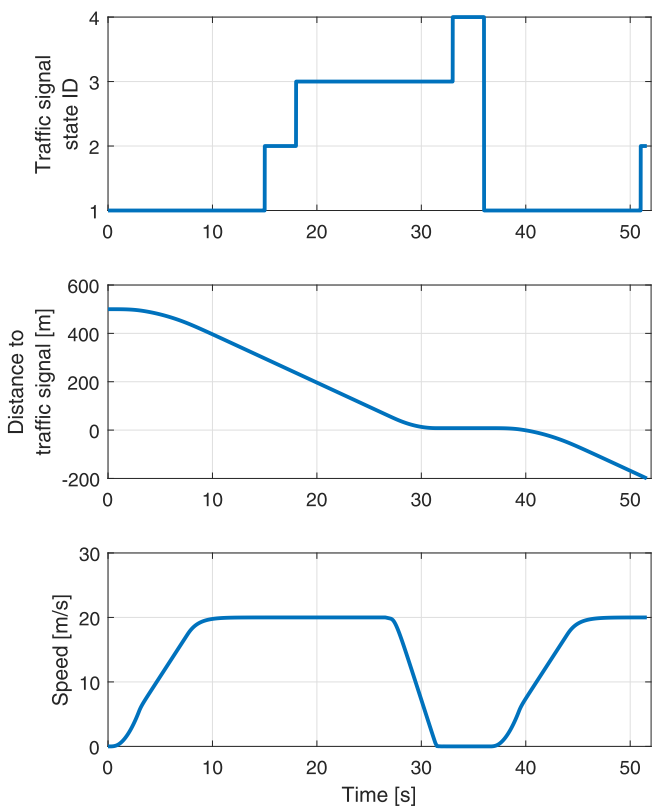

Fig. 19. The traffic signal state ID, and the host vehicle's distance to traffic signal and speed during a simulation without a preceding vehicle, where the host vehicle uses the IPG CarMaker driver model and the initial traffic signal state is green.

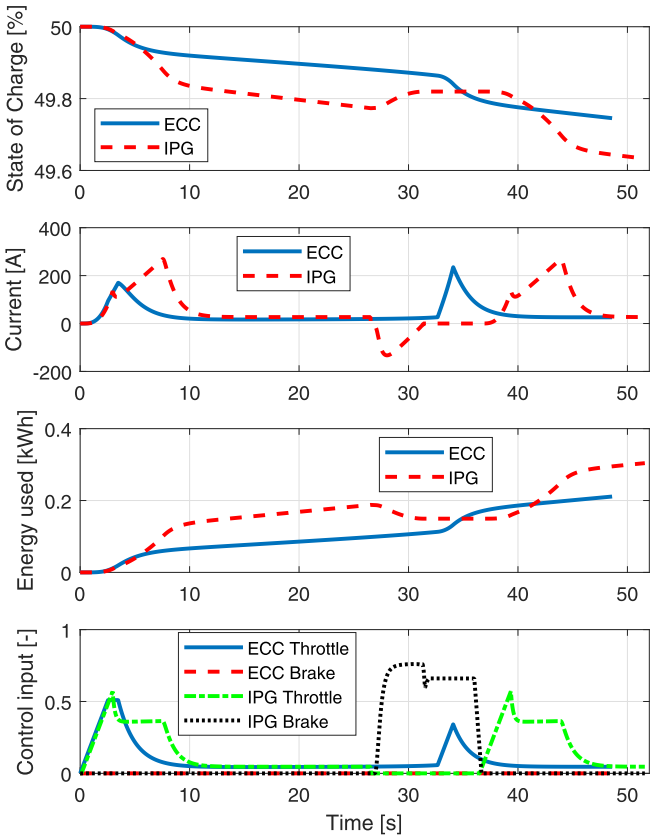

Fig. 20. Performance comparison of the proposed ECC with the IPG CarMaker driver model during a simulation without a preceding vehicle, where the initial traffic signal state is green.

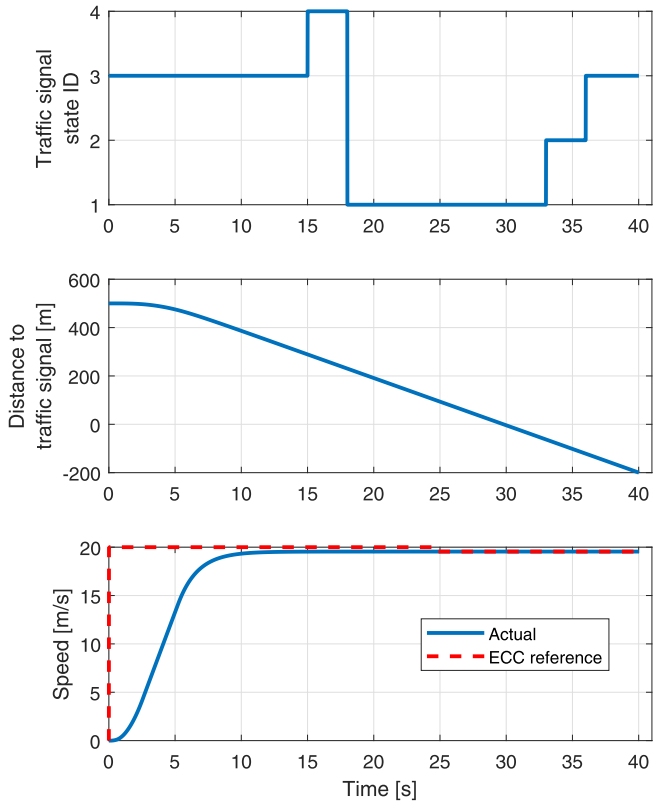

Fig. 21. The traffic signal state ID, and the host vehicle's distance to traffic signal, speed and the speed reference during a simulation without a preceding vehicle, where the host vehicle uses the proposed ECC and the initial traffic signal state is red.

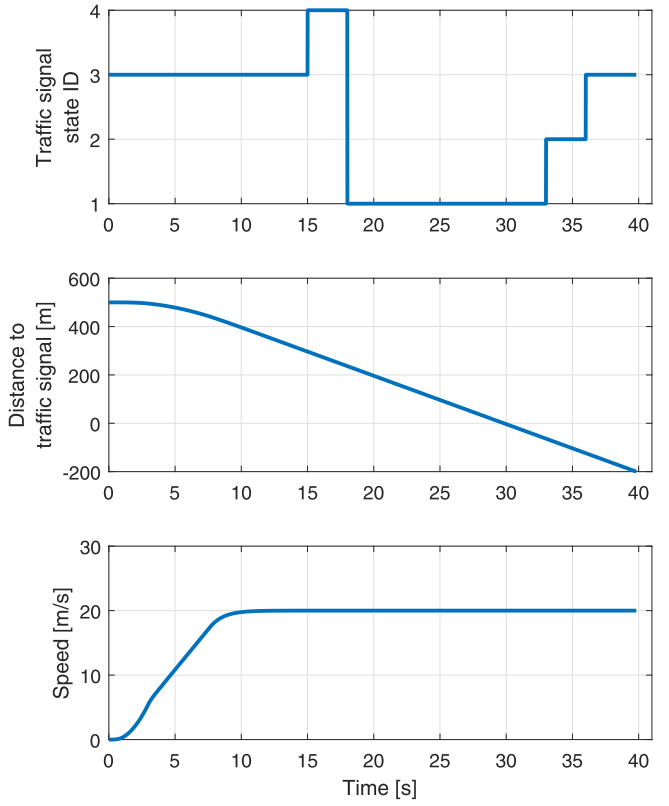

Fig. 22. The traffic signal state ID, and the host vehicle's distance to traffic signal and speed during a simulation without a preceding vehicle, where the host vehicle uses the IPG CarMaker driver model and the initial traffic signal state is red.

host vehicle with IPG CarMaker driver model initially accelerates from standstill to 20 m/s speed (Fig. 19).

- In the ECC case, when the distance to the traffic signal approaches 0 m (Fig. 18), the traffic signal state is green (state ID 1) without the host vehicle decelerating. On the other hand, the host vehicle with IPG CarMaker driver model has to decelerate to standstill while the distance to the traffic signal approaches 0 m so that the traffic signal status becomes green (Fig. 19).
- Before the distance to traffic signal becomes 0 m, the speed of the host vehicle with ECC does not vary much (Fig. 18) and does not become as high as the IPG CarMaker driver model case. On the other hand, the host vehicle with IPG CarMaker driver model initially accelerates to 20 m/s and later decelerates to 0 m/s (Fig. 19).
- The unnecessary acceleration in the IPG CarMaker driver model case causes high electric current above 200 A. Using ECC on the other hand, the electric current stays below 200 A before the traffic signal (Fig. 20). As mentioned before, high electric current is known to reduce an electric vehicle's battery pack efficiency and life span.
- Using the proposed ECC, the battery pack's State of Charge (SOC) reduction is lower than the IPG CarMaker driver model case (Fig. 20) at the end of the 700 m drive.
- Using the proposed ECC, the electric energy consumption is lower than the IPG CarMaker driver model case (Fig. 20) at the end of the 700 m drive. This means the proposed ECC improves the electric vehicle's energy efficiency.
- Briefly around 38 s, the IPG CarMaker driver model case seems to perform better while looking at the SOC reduction or energy used (Fig. 20). However this is not the case as the vehicle speed around 38 s using the IPG CarMaker driver model case is less

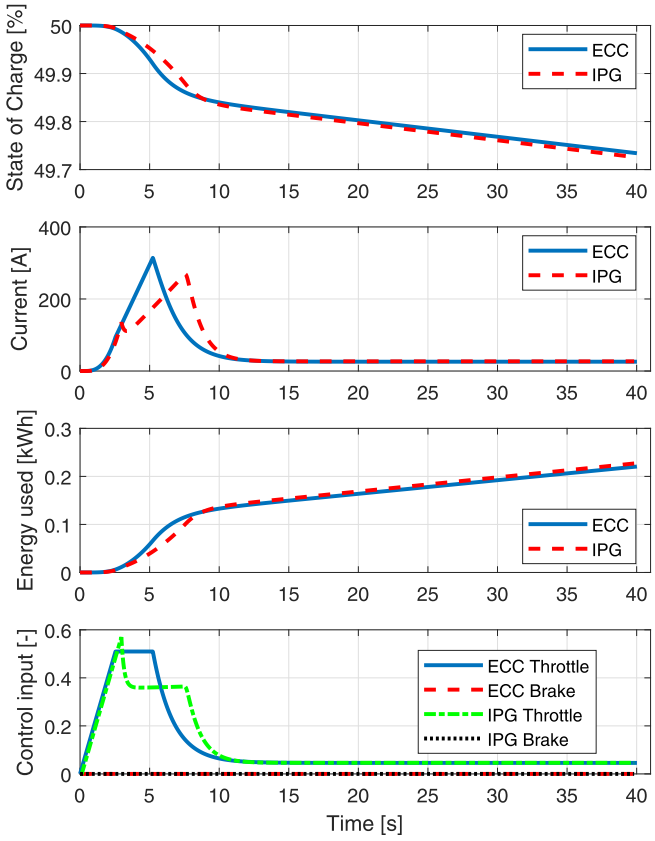

Fig. 23. Performance comparison of the proposed ECC with the IPG CarMaker driver model during a simulation without a preceding vehicle, where the initial traffic signal state is red.

than 5 m/s (Fig. 19), whereas using the ECC, the vehicle speed around 38 s is close to 20 m/s (Fig. 18). This implies considerably higher kinetic energy using the ECC.

In the IPG CarMaker driver model case, as the host vehicle decelerates while approaching the traffic signal, a part of the gained kinetic energy is lost as heat due to friction brakes and only a part of the kinetic energy is recovered using regenerative braking. But using the proposed ECC, kinetic energy is not lost as the vehicle approaches the traffic signal when the traffic signal is green.

Fig. 21 shows the simulation results using the proposed ECC with the initial traffic signal state red. Fig. 22 shows the simulation results using the IPG CarMaker driver model. Fig. 23 shows the simulation results, comparing performance of the proposed ECC against the IPG CarMaker driver model.

From Figs. 21–23, it is seen that the performance using the proposed ECC is approximately same compared to the IPG CarMaker driver model case. This happens because the traffic signal becomes green by chance when the host vehicle reaches the traffic signal.

Table 4 compares the electric vehicle's energy consumption with and without the proposed ECC for all the simulation studies with different initial traffic signal states. Considering all the simulation results shown in Tables 3 and 4, it is seen that the proposed ECC reduces the electric vehicle's energy consumption by approximately 23.56%.

Note that the proposed ECC is not only applicable to electric vehicles but also to vehicles using other energy sources such as diesel, petrol, hydrogen, liquid natural gas, compressed natural gas, etc. This work nevertheless focused on electric vehicle as their widespread acceptance can contribute towards overcoming the challenge of carbon emissions [2,7,12]. One of the main obstacles in their widespread acceptance is range anxiety. Therefore improving energy efficiency and range of an electric vehicle is an important topic.

6. Conclusions

An Efficient Cruise Control (ECC) is proposed in this work to increase the range of an electric vehicle (EV) by controlling the EV's speed with respect to the upcoming traffic signal status. The proposed method prevents an EV from unnecessarily gaining kinetic energy if a part of it has to be dissipated while approaching the upcoming traffic signal. In case there is a preceding vehicle in front of the host vehicle, the ECC maintains a minimum safe inter-vehicular distance from the preceding vehicle.

Model Predictive Control (MPC) theory is used to design and develop the ECC. The proposed method is studied in a simulation environment using MATLAB and IPG CarMaker software packages. The controller is implemented in MATLAB and a Tesla S vehicle model from IPG CarMaker is used to simulate an EV. In the presence of a preceding vehicle, the proposed controller is compared with respect to an Adaptive Cruise Control (ACC), which is also designed and developed using MPC theory so that the comparison is fair. In the absence of a preceding vehicle, the proposed controller is compared with respect to the IPG CarMaker driver model.

Several simulation studies are performed with different initial conditions, and in the presence and absence of a preceding vehicle. The simulation studies have shown that the proposed controller reduces energy consumption of an EV. In the simulations studied in this work, the average energy consumption reduction is approximately 23.56%. This implies that the proposed controller improves an EV's energy efficiency and therefore range, where the latter is an important bottleneck in widespread adoption of EVs.

A limitation of the proposed method is the calculation of remaining time after which the host vehicle can pass through the upcoming traffic signal. In this work, this is done only using the upcoming traffic signal's status signals. However, based on the number of preceding vehicles before the upcoming traffic signal, the calculation of remaining time is not straight forward as one needs to anticipate how long the preceding vehicles will take to accelerate from standstill or low speed. A potential approach could be applying the prediction of queue effects from [20]. This is included in the next steps.

Incorporating the EV powertrain model and a real-time route details in the ECC's MPC formulation can further improve the EV energy efficiency, *e.g.* employing a powertrain model based approach proposed in the patent from Hitachi Ltd, Japan [15] or the optimal energy management method proposed in [5]. Getting necessary permissions from the traffic authority and experimental validation of the proposed method are also important next steps. These directions are recommended for future work.

Acknowledgment

This research was partially funded by EPSRC as part of the Centre for Sustainable Road Freight.

References

[1] B. Asadi, A. Vahidi, Predictive cruise control: utilizing upcoming traffic signal information for improving fuel economy and reducing trip time, IEEE Trans. Control Syst. Technol. 19 (3) (2011) 707–714.
[2] N. Brinkman, M. Wang, T. Weber, T. Darlington, Well-to-wheels Analysis of Advanced Fuel/Vehicle Systems a North American Study of Energy Use, Greenhouse Gas Emissions, and Criteria Pollutant Emissions, Argonne National Laboratory, General Motors and Air Improvement Resource, Inc., 2005.
[3] Driver and Vehicle Standards Agency, "The Offcial DVSA The ory Test for Car Drivers," The Stationery Office, UK, ISBN-13:978-0115534652, 2016.
[4] L.C. Davis, Effect of adaptive cruise control systems on traffic flow, Phys. Rev. E 69 (6) (2004) 066110.

[5] W. Dib, A. Chasse, P. Moulin, A. Sciarretta, G. Corde, Optimal energy management for an electric vehicle in eco-driving applications, Control Eng. Practice 29 (2014) 299–307.
[6] W. Drira, K. Ahn, H. Rakha, F. Filali, Development and testing of a 3G/LTE adaptive data collection system in vehicular networks, IEEE Trans. Intell. Transp. Syst. 17 (1) (2016) 240–249.
[7] R. Edwards, V. Mahieu, J. Griesemann, J. Lariv, et al., Well-to-Wheels Analysis of Future Automotive Fuels and Powertrains in the European Context, SAE Technical Paper, No. 2004-01-1924, 2004, doi:10.4271/2004-01-1924.
[8] L. Guo, B. Gao, Y. Gao, H. Chen, Optimal energy management for HEVs in eco–driving applications using bi-level MPC, IEEE Trans. Intell. Transp. Syst. 18 (8) (2017) 2153–2162.
[9] J.M. Maciejowski, Predictive Control: With Constraints, Prentice Hall, Pearson Education, 2002. ISBN 0-201-39823-0.
[10] A.K. Madhusudhanan, M. Corno, M.A. Arat, E. Holweg, Load sensing bearing based road-tyre friction estimation considering combined tyre slip, Mechatronics 39 (2016) 136–146.
[11] A.K. Madhusudhanan, M. Corno, E. Holweg, Sliding mode-based lateral vehicle dynamics control using tyre force measurements, Veh. Syst. Dyn. 53 (11) (2015) 1599–1619.
[12] J.V. Mierlo, G. Maggetto, Fuel cell or battery: electric cars are the future, Fuel Cells (2) (2007) 165–173.
[13] J. Ploeg, B.T. Scheepers, E.V. Nunen, N.V. de Wouw, H. Nijmeijer, Design and experimental evaluation of cooperative adaptive cruise control, in: Proceedings of the 14th International IEEE Conference on Intelligent Transportation Systems, 2011. Washington, DC, USA.
[14] K. Reif, Adaptive cruise control, in: Fundamentals of Automotive and Engine Technology, Springer Vieweg, Wiesbaden, 2014. Bosch Professional Automotive Information.
[15] S. Sato, N. Tashiro, K. Maki, A. Yokoyama, Running Control Device for Electric Vehicle, Patent No. US 8,744,656 B2, United States Patent, 2014. 3 June.
[16] S.V. Sterkenburg, E. Rietveld, F. Rieck, B. Veenhuizen, H. Bosma, Analysis of regenerative braking efficiency a case study of two electric vehicles operating in the rotterdam area, in: Proceedings of the IEEE Vehicle Power and Propulsion Conference, 2011, pp. 1–6. Chicago, IL.
[17] B.J. Varocky, H. Nijmeijer, S. Jansen, I.J.M. Besselink, R. Mansvelder, Benchmarking of Regenerative Braking for a Fully Electric Car, Report No. D&C 2011.002, Eindhoven University of Technology, 2011.
[18] T. Wilberforce, Z. El-Hassan, F.N. Khatib, A.A. Makky, A. Baroutaji, J.G. Carton, A.G. Olabi, Developments of electric cars and fuel cell hydrogen electric cars, Int. J. Hydrog. Energy 42 (40) (2017) 25695–25734.
[19] Q. Xu, R. Sengupta, Simulation, analysis, and comparison of ACC and CACC in highway merging control, in: Proceedings of the IEEE Intelligent Vehicles Symposium, 2003, pp. 237–242. Columbus, OH, USA.
[20] H. Yang, H. Rakha, M.V. Ala, Eco-cooperative adaptive cruise control at signalized intersections considering queue effects, IEEE Trans. Intell. Transp. Syst. 18 (8) (2017) 1575–1585.